Compact Ejector Thrust Augmentation

Brian Quinn*
Aerospace Research Laboratories, Wright-Patterson Air Force Base, Ohio

Ejectors offer interesting means for resolving problems arising from the additional power requirements of V/STOL aircraft. They are capable not only of turning and augmenting the cruise engine's thrust vector, but their efflux can also serve to control circulation lift. The feasibility of ejector propulsion-lift concepts requires the simultaneous attainment of two conflicting objectives: high performance and compactness. Performance is degraded by losses occurring in the inlet, the primary nozzle, and the duct-diffuser of the ejector. Analytic results identified practical loss trade-offs that led to the design of the ejector's components. Static experiments with independently varied duct and diffuser lengths showed, surprisingly, that skewed flows can be diffused effectively. Augmentation ratios in excess of 1.85 were measured with a duct-diffuser 28 in. long. Increasing the length to 50 in. caused augmentation ratios to exceed 2.0.

Nomenclature

A	= area
c_f	= skin friction coefficient
C_p	= diffuser pressure coefficient
F	= force
h,H	= nozzle spacing (3 in.), ejector span (60 in.)
L	= length; ejector total $L = L_I + L_M + L_D$; duct-diffuser $L = L_M + L_D$
p,P_T,q	= static, total, dynamic pressures ($q = \rho/2\ V^2$)
q	= quality of ejector
$\Delta q/q_{\text{IDEAL}}$	= measure of duct-diffuser losses
S	= spacing between tips of nozzle
$u, V = \int_A u\, d(a/A)$	= velocity at a point, mass averaged velocity
w	= width of ejector at throat (10 in.)
β	= flow skewness or momentum coefficient
η_N	= thrust efficiency of nozzle
θ	= diffuser included angle
ξ_1, ξ_f	= inlet loss coefficient, friction factor
ρ	= mass density
Φ	= static thrust augmentation ratio, Eq. (3)

Subscripts

D,I,M	= diffuser, inlet, mixing duct
isen	= isentropic conditions
0,1,2,3,∞	= primary, entrained or inlet, diffuser entrance, diffuser exit, ambient

Introduction

INSTALLING thrust augmenting ejectors in V/STOL aircraft provides interesting means of matching the installed power requirements of flight with those of takeoff and landing. Additional benefits derive from using the ejector efflux to control and augment forces whose origins are found in aerodynamic circulation. For practical reasons, lift and thrust augmenting ejectors must simultaneously achieve two objectives: high performance and compactness. Laboratory experiments dramatically point out that ejector performance improves as the mixing between the primary and entrained streams becomes more complete. Insofar as complete mixing theoretically requires a very long ejector, the high performance objective conflicts with the compactness objective. This identifies the first of a sequence of conflicting objectives, each of which must be compromised in the design and fabrication of compact, high performance ejectors. Practical solutions to the problems presented by compromises in component design are the subject of this work.

Presented as Paper 72-1174 at the AIAA/SAE 8th Joint Propulsion Specialist Conference, New Orleans, La., November 29–December 1, 1972; submitted December 11, 1972; revision received May 29, 1973.

Index categories: Airbreathing Propulsion, Subsonic and Supersonic; Nozzle and Channel Flow.

*Aerospace Engineer, Energy Conversion Research Laboratory. Associate Fellow AIAA.

Analytical Remarks

The paper[1] from which article originated, extended von Kármán's[2] thrust augmentation analysis to include losses encountered in the primary nozzle, inlet, mixing duct and diffuser. The analysis balanced total impulse and mass flow through the ejector and produced three equations important to the present discussion:

$$(V_1/V_0)^2[2A_1A_2/A_0^2 - (1+\xi_1)(A_2/A_0)^2 - q(A_1/A_0)^2] - 2qV_1A_1/V_0A_0 + 2\beta_0A_2/A_0 - q = 0 \quad (1)$$

$$q = \beta_2[2\xi_f + 2 - C_p] \quad (2)$$

and

$$\phi = F_{\text{ejector}}/F_{\text{isen}} = \beta_3A_0/A_1(1 + A_1V_1/A_0V_0)^2[1/\eta_N^2 - (1+\xi_1)(V_1/V_0)^2]^{-1/2} \quad (3)$$

The first equation expresses the velocity V_1 of the entrained flow as a fraction of the velocity V_0 of the primary flow and relates this ratio to the geometry of the ejector and the losses encountered by the flows. These include an inlet loss coefficient $\xi_1 = \int_{A1} 2\Delta P_T/A_1\rho v_1^2 da$, and the quality q of the ejector, which combines the effects of events that occur downstream from the plane of injection. Equation (2) relates the quality to the degree, β_2, to which mixing between primary and entrained streams has been completed, wall friction $\xi_f = c_f/2(V_{\text{ref}}/V_2)^2A_{\text{ref}}/A_2$, and the pressure coefficient of the diffuser, $C_p = 2(p_3 - p_2)/\rho\beta V_2^2$. How compactness influences performance can be seen in Eq. (2). As the ejector is shortened, mixing becomes less complete and the flow skewness β_2 increases beyond its ideal value of unity. The resulting increase in q reduces the ratio V_1/V_0 thereby degrading the performance of the ejector. For computational purposes it has been found convenient to write $q = q_{\text{IDEAL}}\ (1 + \Delta q/q_{\text{IDEAL}})$ where $q_{\text{IDEAL}} = 1 + (A_2/A_3)^2$ and $\Delta q/q_{\text{IDEAL}}$ is treated as a parameter. Equation (3) defines the static thrust augmentation ratio Φ. As a fundamental measure of ejector performance it relates the thrust produced by the ejector to the thrust generated by an isentropic expansion of the primary mass from the driving pressure P_{T0} to

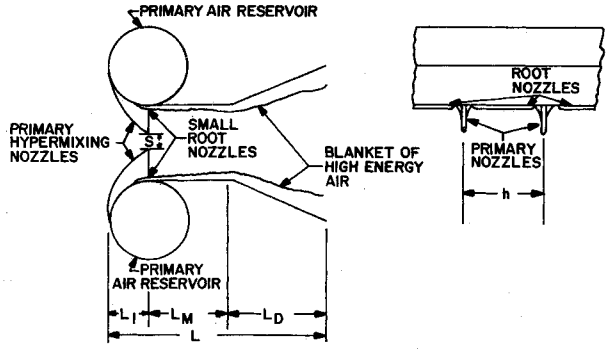

Fig. 1 Schematic diagram of experimental ejector.

ambient pressure P_{T_∞}. The second part of the equation relates augmentation to the geometry of the ejector, its losses, and the velocity ratio V_1/V_0.

Experimental Program

The purpose of the experiments was to demonstrate that losses can be controlled and high performance can be obtained with compact ejectors. The test object was a 60 × 10-in. rectangular throat ejector with a cross section resembling the sketch of Fig. 1. Primary air is discharged from reservoirs through discrete nozzles spaced at approximately h = 3 in. intervals along the H = 60 in. span and through small, flush mounted root nozzles positioned between the primary nozzles. Small amounts of primary air were also admitted through nozzles located on the end walls of the ejector. Secondary air was entrained through an inlet formed by stainless steel panels that were used to mount the primary and root nozzles to the 15-in.-diam reservoirs. Except for several end wall blowing tests, the nozzle and inlet geometries were not varied and are shown to scale in Fig. 2. The contour of the inlet was designed to account for nozzle blockage and provide uniform acceleration of the entrained air up to the plane of injection.

With L_I fixed at 6.5 in. by the inlet design, the remainder of the total length L of the ejector was alloted to a constant area mixing duct of length L_M and to a diffuser of length L_D (Fig. 1). It was argued that the lion's share of the available length should be awarded to the constant area mixing duct. Otherwise, incomplete mixing between primary and secondary streams would present a skewed profile to the diffuser. As diffusion amplifies skewness,[3] the large value of β_2 would degrade augmentation for reasons discussed above. The counter argument noted that large augmentation ratios require large diffuser area ratios. In turn, the relatively small divergence angles of practical diffusers suggest apportioning most of the available length to the diffuser. Lacking enough information to resolve the issue, several combinations of L_M and L_D were tested. Table 1 specifies their dimensions in inches.

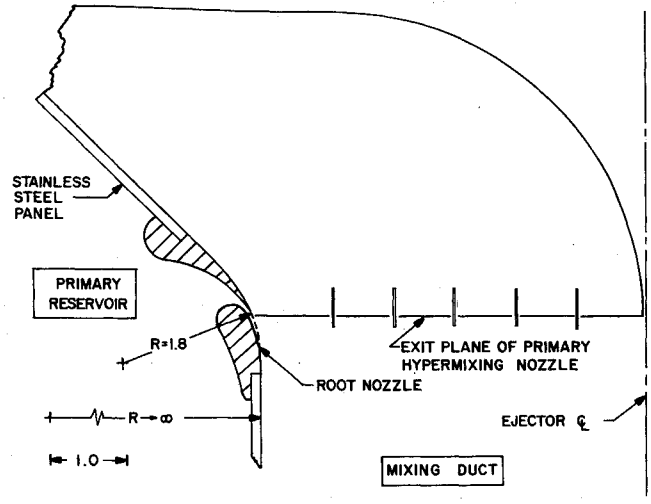

Fig. 2 Diagram of nozzle locations and inlet geometry, to scale.

Diffuser inefficiencies seriously degrade ejector performance through the Δq loss, which they enter through the C_p term in Eq. (2). They arise, partly, through the encounter of a low energy boundary layer with the attendant adverse pressure gradient and can frequently be read in the pattern of the flow. Depending on geometric and fluid dynamic properties, diffuser flows assume a variety of characters that approach the one-dimensional idealization in the one extreme and completely separated slug flow in the other. The diffusers tested in these experiments were observed to produce streamwise vortices in the corners formed by the juncture of the end walls and the side walls of the diffusers. The dimension of the vortices grew in the downstream direction and their sense of rotation provoked flow separation on the end walls. This contribution to the Δq loss was controlled by energizing the end walls with a small quantity of primary fluid provided by the twelve small nozzles shown in Fig. 3. In addition, the losses arising on the side walls of the diffuser, especially at large divergence angles, were controlled by the blanket of high energy air sketched in Fig. 1. By scrubbing the walls of the duct-diffuser with part of the more kinetic primary fluid, this first of two services provided by the small root nozzles increased the friction loss ξ_f, but not by enough to override the benefits of more efficient diffusion. The second task addressed by the root nozzles controlled inlet losses ξ_1. Near the exit of the primary nozzle the radius of curvature of the inlet contour increases rather abruptly from R = 1.80 in. to $R \to \infty$ as shown in Fig. 2. In passing from the inlet to the duct, centrifugal components of the entrained momentum are converted into local increases in pressure. The root nozzles energize the boundary layer and enable it to negotiate the locally adverse pressure gradient without separating and increasing ξ_1. The integration of pressures surveyed in a separate experiment indicated $\xi_1 = 0.025$ for the inlet shown in Fig. 2.

In the absence of separation, inlet losses appertain mostly to skin friction and are thus sensitive to the area scrubbed by the entrained flow. But attempts at reducing the size and number of the primary nozzles for the sake of reducing their wetted area must be tempered by the more important objective of thoroughly mixing entrained and primary streams. Simply stated, good mixing means that turbulence has distributed the momentum of the primary fluid more or less uniformly across a plane normal to the direction of the mean flow. In other words, primary jets from each side have penetrated to the center of the ejector and adjacent jets have spread and merged.

Unfortunately, several investigators[4-6] have shown that

Table 1. Dimensions of duct diffusers in inches

Configuration	L_M	L_D	$L = L_M + L_D$
A	13	32.35	45.25
B	13	15.25	28.25
C	5	23	28
D	16	34	50
F	5	45	50
H	5	45[a]	50

[a] Configuration H had a compound diffuser. The first 14 in. of L_D diverged at an included angle of 36°, the remainder used to obtain the required A_3/A_2.

the length characterizing the longer dimension of a finite aspect ratio jet at first shrinks, then eventually grows with downstream distance. A shrinking jet can obviously not penetrate. Inclining the nozzles would provide better penetration, but the tilt loss, β_0, contraindicated this approach. Instead, the primary nozzles were designed to span the complete width of the ejector and virtually reduce the dimension S (Fig. 1) to zero. In practice, however, a manufacturing error at the root canted the nozzles, (Fig. 3) and caused a slight separation between nozzle tips.

The spacing h between adjacent nozzles relates to the length of the ejector and the spreading rate of confined turbulent jets in a coflowing stream. Increasing the spread rate has the effect of reducing inlet losses by reducing the number of primary nozzles. For this reason, a continuing effort has been made to develop efficient nozzles that produce very rapidly spreading jets. These have been called hypermixing jets and nozzles. While most of this work remains unreported at present, some aspects can be found in Refs. 5, 7-9.

A three-quarter view of the hypermixing nozzle used in the present experiments can be seen along with the small root nozzle, in Fig. 4. Both were injection molded from a Nyafil material. The cross section of the primary nozzle was distributed to present a symmetrical airfoil of 18% maximum thickness to the entrained air. It was felt that reducing the thickness of the nozzle would degrade its thrust efficiency η_N, which separate tests determined to be 96%. The segmented exit plane of the primary nozzle is suspected of generating a system of streamwise vortices that entrain additional fluid into the turbulent jet, thereby accelerating its spreading rate. While difficult to measure precisely, the design exit area of the primary nozzle was 0.5 in.^{2} That of the root nozzles was 0.0915 in.^{2} The design area ratio of the ejector configured with 38 primary nozzles, 40 root nozzles, and both sets of end wall nozzles

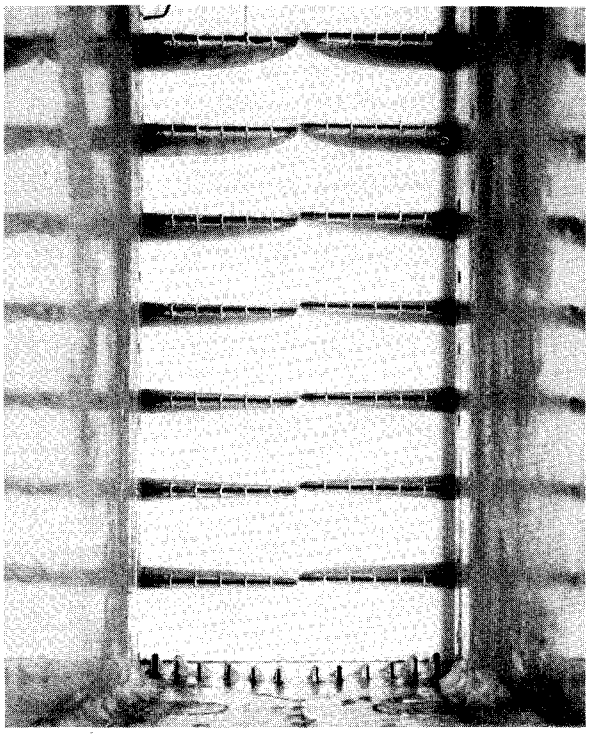

Fig. 3 View of nozzles from inside the diffuser, looking upstream. The small misalignment in the tips of the hypermixing nozzles is due to a manufacturing error. Root nozzles cannot be seen. The twelve small nozzles spray primary air across the end wall. The fillets were formed from modeling clay.

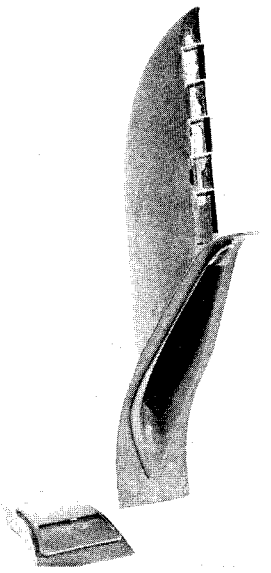

Fig. 4 Three-quarter view of primary hypermixing nozzle and small root nozzle.

was thus

$$A_1/A_0 = A_2/A_0 - 1 = \{60(10)/[38(.5) + 40(.0915) + 2(.5)]\} - 1 = 24.36$$

The completely assembled apparatus can be seen in Fig. 5. The ejector is suspended by cables from a steel framework and provided with primary air by the ducts shown running from the left, below the ejector. A calibrated orifice plate located within the supply duct meters the flow rate of the primary air, while probes and thermocouples in the reservoirs measure its thermodynamic properties. A load cell measures the thrust F of the ejector and supplies the last item required to compute the augmentation ratio:

$$\Phi = F/\dot{m}_0(V_{\text{isen}}) \tag{4}$$

where $\dot{m}_0$ is the flux of mass passing through the primary, root and end wall nozzles and V_{isen} is the velocity that would result from an isentropic expansion of air from the reservoir pressure to barometric pressure.

A second, independent but concurrent means of computing Φ was provided by a static pressure probe positioned at the plane of injection. When referred to barometric pressure, the information obtained from the static pressure probe, together with the reservoir pressure, was sufficient to compute the ratio of the entrained to primary flow velocities V_1/V_0. Knowing the geometric properties of the ejector, the nozzle efficiency η_N, and the inlet loss coefficient ξ_1, the second part of Eq. (3) was used to compute Φ under the assumption of complete mixing, $\beta_3 = 1$. The computation is considered less reliable than reduction by Eq. (4) because of the complete mixing assumption and its reliance on information obtained at a single point in the ejector. Agreement between the two computations nevertheless adds an additional degree of reliability to the results.

Each of the configurations listed in Table 1 was tested at several diffuser area ratios A_3/A_2 between 1.0 and 2.2. A typical test at a given diffuser setting involved recording experimental parameters at 16 different levels of reservoir pressure P_{T0} between 0 and 8 in. Hg above ambient. A more detailed account of the instrumentation and test procedure followed in these experiments can be found in Ref. 8, in which ejector experiments using nozzles similar to those shown in Fig. 4 are reported.

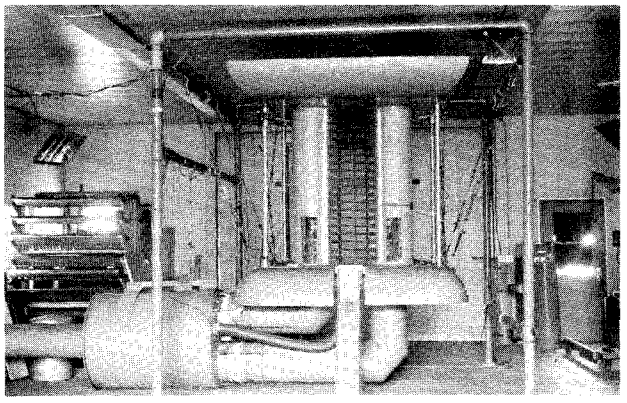

Fig. 5 The completely assembled apparatus and test strand.

Experimental Results

Effects of Pressure Ratio

A question frequently put to ejector experimenters asks if thrust augmentation varies with pressure. The experimental results plotted in Fig. 6 are typical of all the test data and provide the answer. No point deviates from the dashed line indicated the average by more than 2%, and no trend can be observed. Drummond and Gould[10] arrived at a similar conclusion, although small, adverse effects of primary pressure on augmentation have been observed at very high pressure ratios.[11,12]

Effects of Diffusion

The benefits of good diffusion can be seen in Figs. 7–13 which plot augmentation ratio as a function of diffuser area ratio A_3/A_2. Each of the curves shows a characteristic rise in augmentation that eventually peaks and falls as diffusion increases. During the rise in augmentation, entrainment benefits from reductions in q brought about by C_p in Eq. (2). This persists until β_2, friction and diffuser losses eventually limit the entrained mass flux, as shown by the measured values of V_1/V_0 in Fig. 7. The figure also compares the values of thrust augmentation computed by the data reduction Eq. (4), with those computed by assuming $\beta_3 = 1.0$, $A_1/A_0 = 24.3$, $\eta_N = 0.96$, and $\xi_1 = 0.025$ in Eq. (3). Increased diffusion typically tends to magnify the differences between the two calculations, no doubt because skewness develops and β_3 increases beyond the assumed value of one. The remainder of the figures omit V_1/V_0 and the Φ it implies for the sake of space and clarity.

The data obtained with configurations A and B, each with 13-in. mixing ducts, are contrasted in Fig. 8 and clearly demonstrate the advantage of the longer diffuser. The message persists in Fig. 9 which presents the data from testing configurations C and F, each of which had 5-in. mixing ducts. The result is hardly surprising since for a fixed throat W and diffuser ratio A_3/A_2, longer diffusers reduce the diffuser angle and thus, the losses. Very surprising however, is that configuration C with its shorter duct and diffuser, performs as well as, if not slightly better than, configuration A. Configuration A was the design point of the program. On the basis of special experiments with hypermixing nozzles, it was computed that the primary jets would merge 13 in. downstream of the plane of injection. Very recent, still incomplete measurements of the flowfield within the ejector have substantiated the calculation. The attempt to maximize performance by gently diffusing a well mixed flow met with failure. Equally good performance resulted from rapidly diffusing a poorly mixed flow.

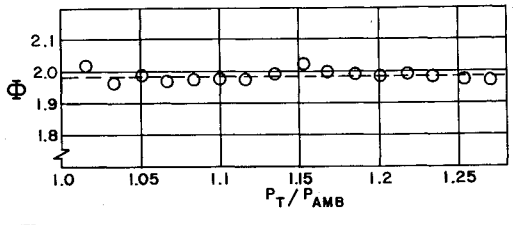

Fig. 6 Thrust agumentation performance of configuration F, $A_3/A_2 = 2.2$ as a function of primary pressure ratio $P_{T0}/P_{T\infty}$.

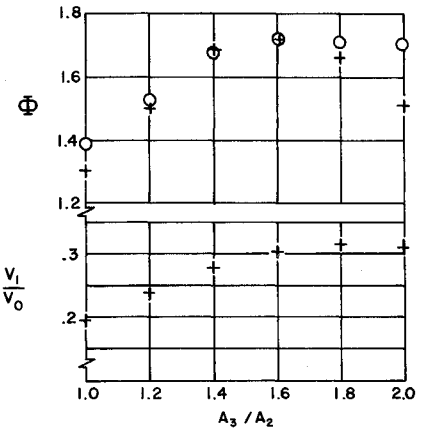

Fig. 7 Measured values of V_1/V_0 and thrust augmentation ratio ϕ for configuration D. The crosses in the upper graph represent ϕ computed from the second part of Eq. (3) with $\beta_3 = 1$, $A_1/A_0 = 24.3$, $\eta_N = 0.96$, $\xi_1 = 0.025$.

The following two Figs., 10 and 11, emphasize allocating the available length to the diffuser. Configurations B and C have nearly equal total lengths, as also do configurations D and F, and in each case the configuration with the shorter mixing duct out performs the other. Mechanical constraints regretably prevented our testing an ejector with no constant area mixing duct.

Since the above observations imply a reduction in skewness during diffusion, they would seem to be at odds with the generally accepted view to the contrary. However, subsonic, skewed flows are rarely diffused by expanding the channel in a direction normal to the sense of skewness, as in this ejector. Usually, as in Ref. 3, the breadth of the channel is increased in the same sense as the flow is skewed. The circumstances under which nonuniform flows can be diffused efficiently deserve considerable attention.

Friction Effects

Skin friction losses appear to be very small since the performance of configurations B and C with no diffusion differs negligibly from that of the considerably longer configurations D and F. Note, however, that the shorter mixing ducts might also promote better diffusion by extracting less momentum from the energy blanket set down by

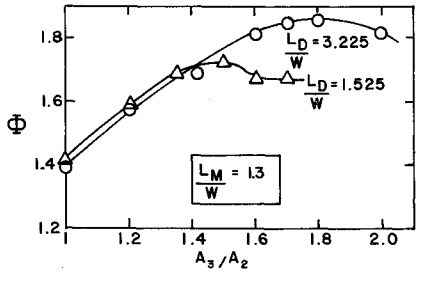

Fig. 8 Thrust augmentation data for configurations A,○ and B,△.

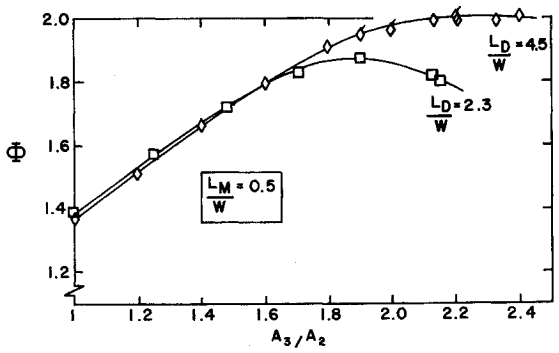

Fig. 9 Thrust augmentation data for configurations *C*, □ and *F*, ◇.

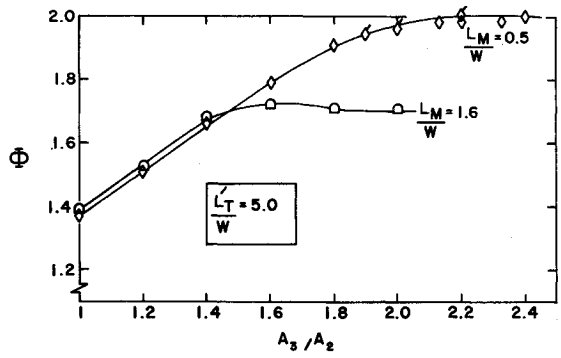

Fig. 11 Thrust augmentation data for configurations *D*, ○ and *F*, ◇.

the root nozzles. In designing the compound diffuser of configuration *H*, it was reasoned that the small losses sustained in flowing through a short duct would enable the energy blanket to encounter a very abrupt diffuser angle without separating. The data obtained with configuration *H* are presented along with those from configuration *F*, from which *H* evolved, in Fig. 12. The merits of the compound diffuser are debatable: it obviously provoked losses in addition to those in the straight wall diffuser over a substantial range of diffuser area ratios. Only for A_3/A_2 greater than around 2.3 can any benefit be observed, and this only extends the peak value of Φ from 2.0 to 2.06.

End Wall Energization

The effects of end wall blowing, Fig. 13, are far more dramatic. The small nozzles shown in Fig. 4 spray less than 5% of the total primary mass along the end walls. But when deprived of this energization, losses ruin the performance of what had been a good thrust augmentor. Nor is performance determined by the quantity of blowing alone. A single nozzle, capable of supplying almost twice as much air, replaced the twelve small nozzles on each of the end walls. This design was less able to distribute the flow uniformly across the end wall and was less successful in achieving very high levels of thrust augmentation.

Accuracy and Repeatability

The author estimates the accuracy of the thrust augmentation data at 97%, or better. This figure derives mostly from the use of very simple instruments, frequently calibrated. The repeatability of the experiments is evidenced by the agreement between the data of the five basic configurations at low diffuser area ratios and by the flagged symbols in Figs. 9 and 11. These data were obtained after configuration *F* had been disassembled, replaced by *D*, *G*, and *H*, and then reassembled a month later.

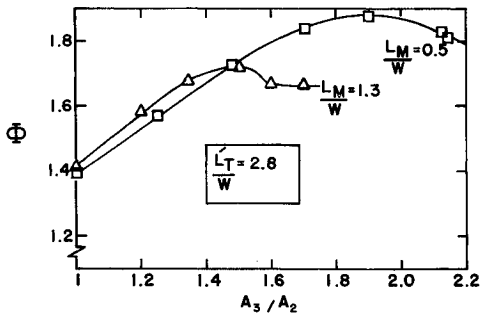

Fig. 10 Thrust augmentation data for configurations *B*, △ and *C*, □.

The Δq Loss

Equations (1) and (3) can be used to predict ejector performance if ξ_1, η_N, β_0 and $\Delta q/q_{IDEAL}$ can be estimated reasonably. In this regard, Δq presents the most difficulty since it combines the effects of friction, mixing and diffusion and since experience and handbooks can be brought to bear on the others, provided, of course, the flows remain attached. Insight into the variation of Δq with diffuser half-angle is provided by Fig. 14. The curves were constructed by substituting the experimental values of ξ_1, η_N, β_0 and Φ into Eqs. (1) and (3) and numerically solving for $\Delta q/q_{IDEAL}$. The curves give the appearance of decreasing linearly with the sine of the diffuser half angle, at a rate determined by the configuration, specifically L_M/W. This trend persists until a threshold value is reached, whereupon $\Delta q/q_{IDEAL}$ remains fixed. That the five configurations have nearly the same threshold value will assist further predictions. The applicability of these results to completely different designs employing central primary injection[7,13] is indicated by the crosshatched region of the figure. The ejectors used in Refs. 7 and 13 experiments include a range of inlet area ratios between 4 and 8.6, far different from 24, the inlet area ratio of the present experiments.

Conclusions

In summary, the experiments have shown:

1) Good agreement between two independent techniques for computing thrust augmentation ratios. This, together with the repeatability of the experiments, furthers confidence in the rather high augmentation values that were measured.

2) The efficiency of abrupt ejector inlets can be maintained at reasonable levels if a small part of the primary fluid can be used to energize inlet boundary layers. Reducing the inlet loss coefficient ξ_1 from the value of 11%

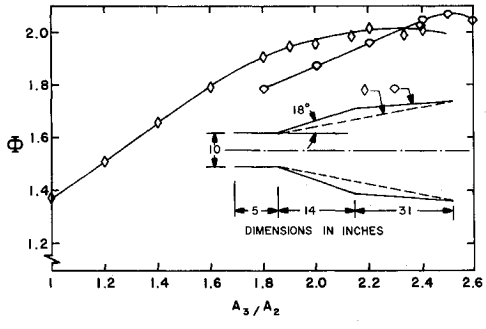

Fig. 12 Differences in augmentation ratio φ obtained with the straight wall diffuser of configurations *F*, ◇ and the compound diffuser of configuration *H*, ○.

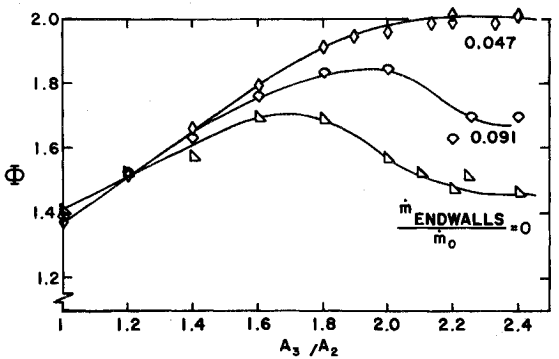

Fig. 13 The effects of end wall blowing on configuration *F*.

found in Ref. 7 to the present value of 2 1/2% can be ascribed, to a large extent, to the root nozzles used in these experiments.

3) Very high diffusion rates can be achieved by covering the walls of an ejector with a blanket of high energy primary fluid. Whereas other investigators[7,10,11] have found augmentation ratios to peak at diffuser half angles less than 5 or 6°, the highest augmentation ratios occur at approximately 10° in the present experiments. Larger optimum diffuser angles are also reported[12] with ejectors that use Coanda injection schemes.

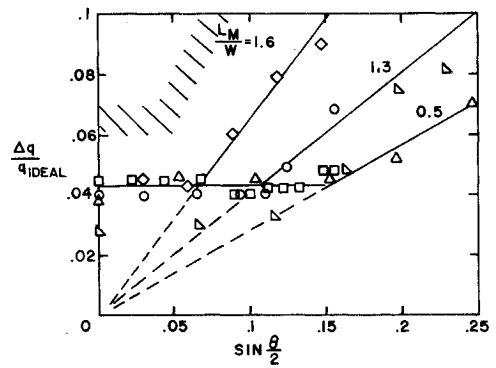

Fig. 14 Experimentally implied values of $\Delta q/q_{IDEAL}$ for configurations *A*,○; *B*,△; *C*,△ and *F*,□. Shaded region includes data from Refs. 7 and 13.

4) Analytical results indicate that ejector performance is very sensitive to the losses of its components. The loss in thrust augmentation increases on nearly a 1:1 basis with ξ_1, η_N, and β_0 and on a 2:1 basis with $\Delta q/q_{IDEAL}$ losses, approximately.

Most important of all, the high levels of static thrust augmentation achieved with compact ejectors in these tests removes the first, and most debilitating, impediment to proving the feasibility of ejector propulsion-lift systems for V/STOL aircraft.

References

[1]Quinn, B., "Recent Developments in Large Area Ratio Thrust Augmentors," AIAA Paper 72-1174, New Orleans, La., 1972.

[2]von Kármán, T., "Theoretical Remarks on Thrust Augmentation," *Reissner Anniversary Volume Contributions to Applied Mechanics*, J. W. Edwards, Ann Arbor, Michigan, 1949.

[3]Hill, P. G., Schaub, U. W., and Senoo, Y., "Turbulent Wakes in Pressure Gradients," *Transactions of the ASME: Journal of Applied Mechanics*, Vol. 85, Dec. 1963, pp. 518–524.

[4]Trentacoste, N. and Sforza, P. M., "Further Experimental Results for Three-Dimensional Free Jets," *AIAA Journal*, Vol. 5, No. 5, May 1967, pp. 885–891.

[5]Eastlake, C. N., "The Macroscopic Characteristics of Some Subsonic Nozzles and the Three Dimensional Turbulent Jets They Produce," Rept. ARL 71-0058 (AD 728676), 1971, Aerospace Research Labs., Wright-Patterson Air Force Base, Ohio.

[6]Viets, H., "The Three Dimensional Laminar Elliptical Jet in a Coflowing Stream," Rept. ARL 72-0042 (AD 754227), 1972, Aerospace Research Labs., Wright-Patterson Air Force Base, Ohio.

[7]Fancher, R. B., "Low-Area Ratio, Thrust Augmenting Ejectors," *Journal of Aircraft*, Vol. 9, No. 3, March 1972, pp. 243–248.

[8]Quinn, B., "Experiments with Hypermixing Nozzles in an Area Ratio 23 Ejector," Rept. ARL 72-0084 (AD 752207), 1972, Aerospace Research Labs., Wright-Patterson Air Force Base, Ohio.

[9]Bevilaqua, P. M., "An Eddy Viscosity Model for Hypermixing Wakes and Jets," Rept. ARL 72-0047 (AD 743297), 1972, Aerospace Research Labs., Wright-Patterson Air Force Base, Ohio.

[10]Drummond, A. M. and Gould, D. G., "Experimental Thrust Augmentation of a Variable Geometry, Two-Dimensional Central Nozzle Ejector," NRC Rept. LR-328, 1962, National Aeronautical Council, Ottawa, Canada.

[11]Johnson, J. K. et al., "Steady Flow Ejector Research Program," Final Report Extended Contract Nonr-3067(00), AD 263 180, 1961, Lockheed Aircraft, Marietta, Ga.

[12]Ambrosiani, J. et al., "Lift Augmenting Ejectors for V/STOL Aircraft," Rept. NR 71H-532, 1972, North American Rockwell, Columbus, Ohio.

[13]Campbell, J. M., Lawrence, R. L., and O'Keefe, J. V., "Design Integration and Noise Studies for Jet STOL Aircraft," Vol. III, CR 114285, May 1972, NASA.